Triphase Microfluidics

DOI: 10.1002/anie.201107126

Triphase Microfluidic-Directed Self-Assembly: Anisotropic Colloidal Photonic Crystal Supraparticles and Multicolor Patterns Made Easy**

*Ziyi Yu, Cai-Feng Wang, Luting Ling, Li Chen, and Su Chen**

The self-assembly of colloidal particles opens novel avenues for the generation of functional materials with collective optical, elctronic, and magnetic properties.[1] Particularly, colloidal photonic crystal (CPC) materials which are created by the self-assembly of monodispersed colloidal particles often show unique optical properties beyond those of their single components, such as diffractive light abilities and photonic bandgaps.[2] Microfluidic devices have recently emerged as a powerful playform to engineer CPCs with diverse strutures,[3] high stabilities,[4] monodisperse sizes,[5] and functionalization,[6] allowing them to meet the requirments for practical applications ,such as biological analysis,[7] optical devices,[8] and chemical sensors.[9] However, it is still a great challenge to mount or shape CPCs into a desired morphology (e.g., spheres, Janus, ellipsoids, and dumbbell-like supaparticles); efficient pathways are needed to selectively endow CPCs with versatile functions whilst preserving their original optical properties.

Herein, we developed a triphase microfluidic-directed self-assembly to construct CPC supraparticles with controllable and predictable shape, and selectively introduced advanced functions to them. The triphase microfluidic technique is a co-flowing system that produces continuous microdroplets comprising two immiscible phases. By adjusting the interfacial tension of each phase in the microfluidic system, CPC supraparticles with tunable shape, varying from crescent, meniscus, and ellipsoid to spherical were prepared by the self-assembly of the monodisperse colloidal particles in these microdroplet templates. Importantly, studying the interface chemistry indicated that the structure of the biphasic microdroplets and the resulting CPCs might be predicted in our strategy. The further introduction of photoinduced consolidation into the triphase microfluidic system yielded core–shell or Janus CPC superstructures. The encapsulation of magnetic nanoparticles created Janus CPC supraparticles with superparamagnetism and a photonic bandgap in two distinct hemispheres. These multifunctional Janus CPC supraparticles exhibit "Dark" and "Light" switchable behaviors under an external magnetic field, and thus can be processed into rewritable and color-tunable photonic patterns. To our knowledge, this is the first example of the utilization of the triphase microfluidic technique for the design of anisotropic CPCs. This facile strategy can be extended to build up a series of novel multidimensional colloidal structures, with the aim of collecting colloidal particles and orgnizing them into functional materials for pratical application.

Figure 1 a illustrates the fabrication of shape-controllable CPC supraparticles in a triphase microfluidic flow-focusing device composed of a cylindrical polydimethylsiloxane (PDMS) capillary and a pair of inner cylindrical 25G steel needles. We chose three immiscible fluids, an aqueous solution of monodisperse polystyrene (PS) microspheres in

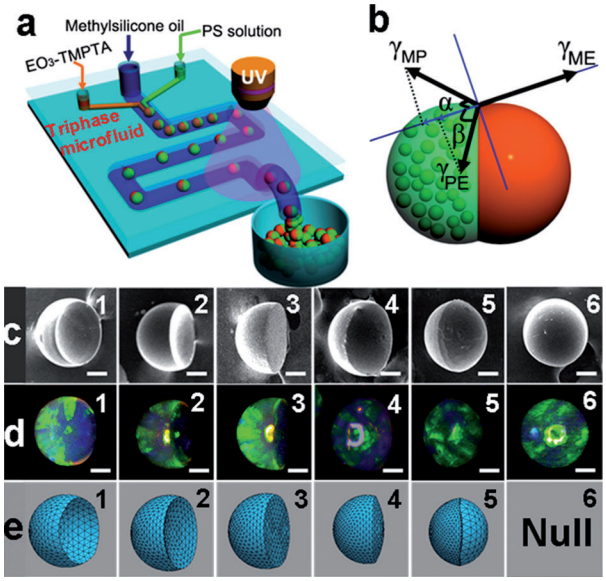

Figure 1. a) Schematic representation of the triphase microfluidic device. A UV beam is applied over the downstream area of the PDMS capillary for the fabrication of core–shell and Janus CPC supraparticles. b) Schematic illustration of the balancing of the three interfacial tensions and the formation of CPC supraparticles [see text and Eqs (1) and (2) for details]. Scanning electron microscope (SEM) images (c) and optical microscope images (d) of various shapes of CPC supraparticles, formed with different concentrations of Triton X-100 (see text for details) . e) Surface Evolver simulation of PS compartment in biphasic droplets based on calculations of the three interfacial energies. The scale bars in (c) and (d) are 50 μm.

[*] Z. Y. Yu, Dr. C. F. Wang, L. T. Ling, Prof. L. Chen, Prof. S. Chen
State Key Laboratory of Materials-Oriented Chemical Engineering and College of Chemistry and Chemical Engineering, Nanjing University of Technology
Nanjing 210009 (P.R. China)
E-mail: chensu@njut.edu.cn

[**] This work was supported by the National Natural Science Foundation of China (21076103, 21006046 and 21176122), National Natural Science Foundation of China-NSAF (10976012), the Specialized Research Fund for the Doctoral Program of Higher Education of China (20103221110001), the Colleges and Universities in Jiangsu Province Plans to Graduate Research and Innovation (Grant CX10B_180Z), and the Priority Academic Program Development of Jiangsu Higher Education Institutions (PAPD).

Supporting information for this article is available on the WWW under http://dx.doi.org/10.1002/anie.201107126.

one needle, a photopolymerizable monomer trimethylolpropane ethoxylate triacrylate (EO_3-TMPTA) in the other needle, and methylsilicone oil in the PDMS capillary, respectively. At the tip of the pair of needles, the flows of PS solution and EO_3-TMPTA can be broken by the continuous phase of methylsilicone oil and then incorporated into uniform biphasic droplets. The geometry of biphasic droplets arises from the minimization of the interfacial free energies which can be estimated by Young–Dupre's equations [Eq. (1) and (2)][10]

$$\gamma_{ME} = \gamma_{MP}\cos\alpha + \gamma_{PE}\cos\beta \quad (1)$$

$$\gamma_{MP}\sin\alpha = \gamma_{PE}\sin\beta \quad (2)$$

where γ_{ME} is the interfacial tension between methylsilicone oil and EO_3-TMPTA, γ_{MP} is the interfacial tension between methylsilicone oil and the aqueous solution of PS microspheres, γ_{PE} is the interfacial tension between the aqueous solution of PS microspheres and EO_3-TMPTA, and α and β are the contact angles depicted in Figure 1 b. By adjusting the three interfacial tensions, stable PS/EO_3-TMPTA droplets with tunable biphasic geometry can be formed. After solvent evaporation, the PS compartment will organize into CPC supraparticles.

To verify shape-controlled synthesis of CPC supraparticles by triphase microfluidics, the PS solution was emulsified by varying the concentration of polyoxyethylene octylphenol ether (Triton X-100), which yielded different interfacial tensions with EO_3-TMPTA and methylsilicone oil, respectively (Supporting Information, Table S1). The velocity of methylsilicone oil (V_M) was set to be 5 mL h^{-1}, and the velocity of PS solution (V_P) and EO_3-TMPTA (V_E) were both set to be 0.15 mL h^{-1}. With Triton X-100 concentration of 0.333 wt % (group 1; $\beta = 11.5°$), the PS solution droplet wetted a portion of the surface of EO_3-TMPTA droplet and formed a concave droplet (Supporting Information Movie S1). The biphasic droplets always kept their original shape even after disturbance by a narrow neck in the downstream of the flow. After water evaporation and hexane washing to remove EO_3-TMPTA, a crescent CPC supraparticle with a green color was obtained (Figures 1 c1 and 1 d1). As the concentration of Triton X-100 decreased from 0.267 to 0.067 wt % (groups 2–5), the value of β increased from 49.8° to 160.7°, and the concaved surface of CPC supraparticles was gradually flattened to yield various morphology from meniscus to ellipsoid (Figures 1 c2–1c5 and 1 d2–1 d5). In the absence of Triton X-100 (group 6), surprisingly, EO_3-TMPTA entirely spread on the surface of PS solution droplets to form stable core–shell droplets (Supporting Information, Movie S2), resulting in completely spherical CPC supraparticles after solvent evaporation and template removal (Figure 1 c6 and 1 d6). This phenomenon indicates that γ_{MP} and γ_{PE} are high enough to redistribute the relative interface energies of the three immiscible fluids without surfactant. As well, the structural evolution of the PS compartment in the bicompartmental droplets was simulated theoretically by using Surface Evolver.[11] However, because of the null of values of α and β, the simulation is invalid for group 6 , but for the other groups the simulated morphologies (Figure 1 e) are in good agreement with those obtained experimentally (Figure 1 c), implying the biphasic distribution geometry of droplets as well as the final morphology of CPC supraparticles prepared by triphase microfluidics can be predicted and controlled to some extent.

To gain further insight into the self-assembly behavior of biphasic droplets in the triphase microfluidic system, the spread behavior was investigated by the spreading coefficient, S [Eq. (3)]

$$S_x = \gamma_{yz} - (\gamma_{xy} + \gamma_{xz}) \quad (3)$$

where γ_{yz} is the interfacial tension between phase y and z.[12] As listed in Supporting Information, Table S1, the spreading coefficient of methylsilicone oil (S_M) was negative in all cases. The PS solution and EO_3-TMPTA never separated but remained coupled in the methylsilicone flow. When the spreading coefficient of EO_3-TMPTA (S_E) was less than zero, EO_3-TMPTA covered a part of the surface of PS droplet to achieve CPC supraparticles as displayed in Figure 1 c2–1 c5; when $S_E > 0$, EO_3-TMPTA spread entirely across the spherical PS solution droplet to give a core–shell structure for biphasic droplets and hence ultimately a completely spherical morphology for CPC supraparticles (Figure 1 c6). Moreover, for $S_E > 0$, the diameter of CPC supraparticles increased as the injection velocity of PS solution increased (Supporting Information, Figure S1).

To fabricate core–shell and Janus CPC supraparticles, the biphasic droplets were exposed under UV beam to photopolymerize EO_3-TMPTA (Figure 1 a). With $S_E = 5.4$ mN m^{-1}, core–shell supraparticles with spherical CPC supraparticles encapsulated in the polymerized EO_3-TMPTA resins shells were obtained. By varying the initial size of the PS microspheres in solution, we could tune the structural color of the CPC supraparticles cores. For instance, red, green, and blue structural colors were observed from the surface of CPC supraparticles for PS microspheres with diameters of 240, 208 and 174 nm, respectively (Figure 2 a–c). The average diameter of the core–shell CPC supraparticles was 520 μm with a coefficient of variation of less than 5 %, revealing nearly perfect uniformity in size distribution. To create Janus CPC supraparticles, we modified the spreading coefficient to vary spreading behavior at $S_E = -2.9$ mN m^{-1}. Meniscus CPC supraparticles were bonded to EO_3-TMPTA resins to form uniform Janus CPC superstructures (Figure 2 d–f), which have a smooth surface over a large area (Figure 2 g and h). Unlike the previous reported Janus balls in which two constituent phases are miscible,[8a,13] this Janus CPC supraparticle has distinct boundaries around their equators (Figure 2 g), providing evidence of negligible diffusive mixing effects. The high-magnification SEM image for the surface junction of Janus supraparticles indicates that the PS spheres mainly form a hexagonal close-packed lattice in the CPC compartment (Figure 2 h), which is responsible for generation of structural color.

Furthermore, the modification of Janus CPC supraparticles with multifunctional properties is crucial for their use in practical applications. Specifically, we conferred Janus CPC

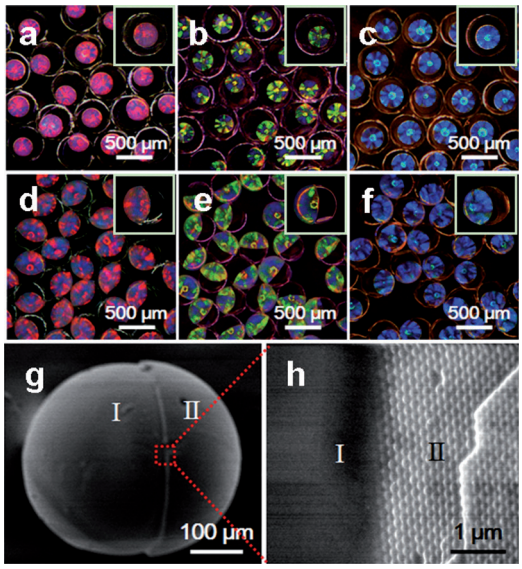

Figure 2. Optical microscope images of a)–c) core–shell and d)–f) Janus CPC supraparticles with differently sized PS microspheres: a,d) 240 nm, b,e) 208 nm, and c,f) 174 nm. g) A SEM image of a typical Janus CPC supraparticle. h) An enlargement SEM image of the equator part of a Janus CPC supraparticle.

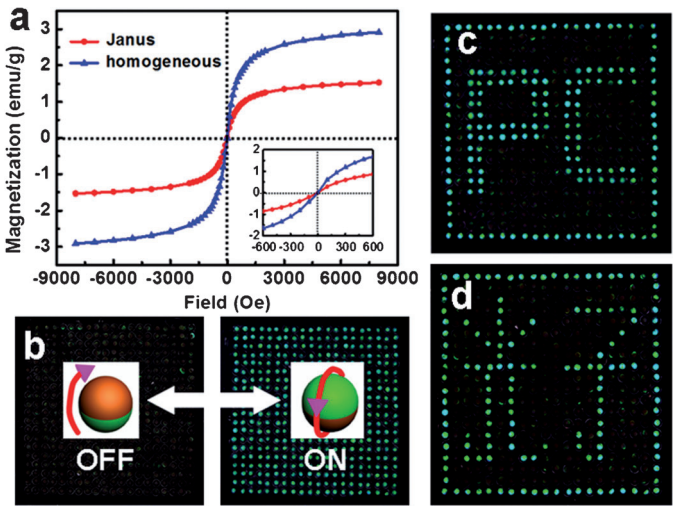

Figure 3. a) Magnetization curves ($T = 300$ K) of homogeneous magnetic EO_3-TMPTA particles and magnetic Janus CPC supraparticles (Inset: expansion showing the absence of hysteresis). b) OFF and ON state of the magnetic Janus CPC supraparticles filled plane substrate. c,d) Optical photographs of the photonic patterns prepared from magnetic Janus CPC supraparticles.

supraparticles with superparamagnetism by directly mixing α-Fe_2O_3 nanoparticles within EO_3-TMPTA hemispheres via photopolymerization. As shown in Figure 3a, the nearly saturated magnetization value for homogeneous magnetic EO_3-TMPTA particles is 2.95 emu g^{-1} under 9 kOe magnetic field at 300 K. While that for α-Fe_2O_3 nanoparticle-doped Janus CPC supraparticles is 1.54 emu g^{-1}, approximately half that of the homogeneous EO_3-TMPTA particles as expected. No hysteresis loop is observed for the magnetization curves, suggesting the presence of superparamagnetism at room temperature (inset in Figure 3a), which enables the micromanipulation of the Janus CPC supraparticles by external fields. By depositing the magnetic Janus CPC supraparticles into highly ordered hole-arrays in a plane substrate and then applying an alternating magnetic field, the Janus CPC supraparticles acquire a dipole moment and rotated freely. As illustrated in Supporting Information, Movie S3, we can catch the movement detail of "Dark" and "Light" switchable behaviors aligned with the direction of the magnetic field, resulting in ON and OFF state (Figure 3b). More interestingly, each Janus CPC supraparticles can act as an independent pixel unit in the multipixel array, which can be micromanipulated by a magnetic needle (Supporting Information, Movie S4). As indicated in Figure 3c, the letters "PC" were successfully freely written in the plane substrate. The writing process is reversible as the pattern displays as soon as a magnetic needle is actuated and returns to the original state immediately after a reverse magnetic stimulation is applied. Therefore, a pattern of Chinese characters translating from photons was also rewritten in the multipixel array (Figure 3d). In contrast to conventional film-type CPCs where the colors are aligned by the film,[14] Janus CPC supraparticle patterns present exceptionally excellent wide viewing angles (Supporting Information, Figure S2). This may be because the optical stop band, derived from spherical CPC superstructure, is independent of the rotation under illumination of the surface. Also, the color and the magnetic property of Janus CPC supraparticle patterns are very stable to light irradiation and long-term storage (Supporting Information, Figure S3).

Another indication is that the magnetoresponsive Janus CPC supraparticles exhibit clear, switchable colors with the application of acrylic acid (AA). Immerged in the aqueous solution of acrylic acid with mass concentrations of 0, 20, 40, 60, 80, and 100 wt %, respectively, Janus CPC supraparticles show diverse stop-band position of 527 (green), 550 (olivine), 574 (yellow), 597 (gold), 623 (orange), and 646 (red) nm, respectively (Figure 4a). We attribute this change to the lattice increase in the CPC supraparticles. As shown schematically in Figure 4b, acrylic acid can infiltrate into the polymeric matrix of PS microspheres to cause swelling, manifested by the increase in both the lattice constant (Table S2) and the diameter of the supraparticle (Figure 4a), which leading to the red-shift of the diffraction peak. The degree of swelling is influenced by acrylic acid concentration, which determines the ultimate range of color tunability. Also, the reversible color transition for CPC suraparticles can be realized because acrylic acid can easily be removed by water rinsing (Supporting Information Figure S4). Benefiting from color adjustment induced by acrylic acid swelling and magnetoswitchable behaviors, we employed Janus CPC supraparticles to flexibly construct multicolored patterns. Typically, when a letter was written by a magnetic needle, an aqueous solution of acrylic acid was utilized as the ink to spray on the Janus PC supraparticles, to restore the color of the letter. We produced multicolor letters of "M" (green), "C" (orange), and "E" (red) patterns under an applied magnetic field by using the aqueous solution of acrylic acid with mass concentration of 0, 40, and 100 %, respectively (Figure 4c). The writing on the substrate confirms that CPC

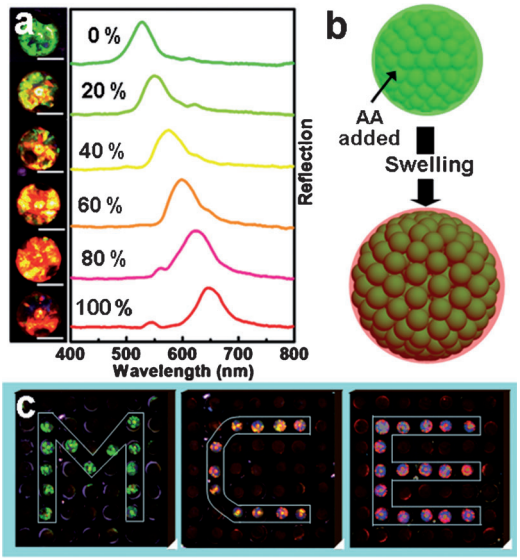

Figure 4. a) Optical microscope images and corresponding reflection spectra of Janus CPC supraparticles with various acrylic acid dosages. b) A schematic illustration for the change of periodic structure of a CPC supraparticle after acrylic acid (AA) swelling. c) Optical photographs of multicolor patterns (see text for details). The scale bars in (a) are 100 μm.

supraparticles can offer promising building blocks for a wide range of applications such as novel color displays, magnetic field sensors, and optical devices.

In summary for the first time, we have successfully established a triphase microfluidic synthesis strategy to allow the directed assembly of monodispersed microspheres into CPC supraparticles. Encouragingly, compared with classical microfluidic methods, this approach shows the unique advance in that the prepared CPC supraparticles are anisotropic in both their geometries and their functions. The shape of CPC supraparticles is tuned from crescent morphology to spherical by simply varying the interfacial tensions in ternary immiscible phases. With photoinduced consolidation, CPC supraparticles are found tightly clinging to the polymer resins and then form core–shell or Janus CPC superstructures. We also demonstrate the micromanipulation of the resultant magnetic responsive Janus CPC supraparticles by appling a magnetic field, forming rewritable full-color photonic patterns. It is reasonable to speculate that this triphase microfluidic directed assembly can be applied not only for fabricating various novel CPC superstructures but also for packing other multifunctional nanocomposite materials.

Received: October 8, 2011
Revised: November 28, 2011
Published online: January 25, 2012

Keywords: colloidal photonic crystals · interfaces · microfluidics · multicolor patterns · self-assembly

[1] a) L. S. McCarty, A. Winkleman, G. M. Whitesides, *Angew. Chem.* **2007**, *119*, 210–213; *Angew. Chem. Int. Ed.* **2007**, *46*, 206–209; b) T. M. Hermans, M. A. C. Broeren, N. Gomopoulos, P. van der Schoot, M. H. P. van Genderen, N. A. J. M. Sommerdijk, G. Fytas, E. W. Meijer, *Nat. Nanotechnol.* **2009**, *4*, 721–726; c) G. A. Ozin, K. Hou, B. V. Lotsch, L. Cademartiri, D. P. Puzzo, F. Scotognella, A. Ghadimi, J. Thomson, *Mater. Today* **2009**, *12*, 12–23; d) O. D. Velev, S. Gupta, *Adv. Mater.* **2009**, *21*, 1897–1905; e) Z. Niu, J. He, T. P. Russell, Q. Wang, *Angew. Chem.* **2010**, *122*, 10250–10265; *Angew. Chem. Int. Ed.* **2010**, *49*, 10052–10066; f) F. Li, D. P. Josephson, A. Stein, *Angew. Chem.* **2011**, *123*, 378–409; *Angew. Chem. Int. Ed.* **2011**, *50*, 360–388; g) S. Yang, C. F. Wang, S. Chen, *J. Am. Chem. Soc.* **2011**, *133*, 8412–8415; h) Z. Yu, C. F. Wang, S. Chen, *J. Mater. Chem.* **2011**, *21*, 8496–8501.

[2] a) D. J. Norris, E. G. Arlinghaus, L. Meng, R. Heiny, L. E. Scriven, *Adv. Mater.* **2004**, *16*, 1393–1399; b) Z. Yu, L. Chen, S. Chen, *J. Mater. Chem.* **2010**, *20*, 6182–6188; c) Y. Zhao, X. Zhao, Z. Gu, *Adv. Funct. Mater.* **2010**, *20*, 2970–2988; d) J. F. Galisteo-López, M. Ibisate, R. Sapienza, L. S. Froufe-Pérez, Á. Blanco, C. López, *Adv. Mater.* **2011**, *23*, 30–69; e) J. Ge, Y. Yin, *Angew. Chem.* **2011**, *123*, 1530–1561; *Angew. Chem. Int. Ed.* **2011**, *50*, 1492–1522; f) J. Wang, Y. Zhang, S. Wang, Y. Song, L. Jiang, *Acc. Chem. Res.* **2011**, *44*, 405–415.

[3] a) S. H. Kim, S. J. Jeon, S. M. Yang, *J. Am. Chem. Soc.* **2008**, *130*, 6040–6046; b) S. H. Kim, S. J. Jeon, G. R. Yi, C. J. Heo, J. H. Choi, S. M. Yang, *Adv. Mater.* **2008**, *20*, 1649–1655.

[4] a) J. H. Moon, G. R. Yi, S. M. Yang, D. J. Pine, S. Bin Park, *Adv. Mater.* **2004**, *16*, 605–609; b) Z. H. Shen, Y. Zhu, L. M. Wu, B. You, J. Zi, *Langmuir* **2010**, *26*, 6604–6609.

[5] a) X. Zhao, Y. Cao, F. Ito, H.-H. Chen, K. Nagai, Y. H. Zhao, Z. Z. Gu, *Angew. Chem.* **2006**, *118*, 6989–6992; *Angew. Chem. Int. Ed.* **2006**, *45*, 6835–6838; b) C. Sun, X. W. Zhao, Y. J. Zhao, R. Zhu, Z. Z. Gu, *Small* **2008**, *4*, 592–596.

[6] a) J. Li, X. W. Zhao, Y. J. Zhao, Z. Z. Gu, *Chem. Commun.* **2009**, 2329–2331; b) J. Li, X. W. Zhao, Y.-J. Zhao, J. Hu, M. Xu, Z. Z. Gu, *J. Mater. Chem.* **2009**, *19*, 6492–6497.

[7] a) Y. J. Zhao, X. W. Zhao, J. Hu, J. Li, W. Y. Xu, Z. Z. Gu, *Angew. Chem.* **2009**, *121*, 7486–7488; *Angew. Chem. Int. Ed.* **2009**, *48*, 7350–7352; b) S. H. Kim, J. W. Shim, S. M. Yang, *Angew. Chem.* **2011**, *123*, 1203–1206; *Angew. Chem. Int. Ed.* **2011**, *50*, 1171–1174.

[8] a) S. H. Kim, S. J. Jeon, W. C. Jeong, H. S. Park, S. M. Yang, *Adv. Mater.* **2008**, *20*, 4129–4134; b) C. Zhu, W. Xu, L. Chen, W. Zhang, H. Xu, Z. Z. Gu, *Adv. Funct. Mater.* **2011**, *21*, 2043–2048; c) O. D. Velev, B. G. Prevo, K. H. Bhatt, *Nature* **2003**, *426*, 515–516.

[9] a) H. Hwang, S. H. Kim, S. M. Yang, *Lab Chip* **2011**, *11*, 87–92; b) T. Kanai, D. Lee, H. C. Shum, R. K. Shah, D. A. Weitz, *Adv. Mater.* **2010**, *22*, 4998–5002; c) T. Kanai, D. Lee, H. C. Shum, D. A. Weitz, *Small* **2010**, *6*, 807–810.

[10] T. Nisisako, T. Torii, *Adv. Mater.* **2007**, *19*, 1489–1493.

[11] a) Y. S. Cho, G. R. Yi, J. M. Lim, S. H. Kim, V. N. Manoharan, D. J. Pine, S.-M. Yang, *J. Am. Chem. Soc.* **2005**, *127*, 15968–15975; b) http://www.susqu.edu/facstaff/b/brakke/evolver/evolver.html (accessed August 2011).

[12] a) P. G. de Gennes, F. B. Wyart, D. Quere, *Capillarity and Wetting Phenomena Drops, Bubbles, Pearls, Waves*, Springer, New York **2004**, p. 16; b) Z. H. Nie, W. Li, M. Seo, S. Q. Xu, E. Kumacheva, *J. Am. Chem. Soc.* **2006**, *128*, 9408–9412; c) S. H. Kim, A. Abbaspourrad, D. A. Weitz, *J. Am. Chem. Soc.* **2011**, *133*, 5516–5524.

[13] S. N. Yin, C. F. Wang, Z. Y. Yu, J. Wang, S. S. Liu, S. Chen, *Adv. Mater.* **2011**, *23*, 2915–2919.

[14] H. Fudouzi, Y. Xia, *Adv. Mater.* **2003**, *15*, 892–896.

